Distributed Formation Control for a Multirobotic Fish System With Model-Based Event-Triggered Communication Mechanism

Shijie Dai, Zhengxing Wu, *Senior Member, IEEE*, Pengfei Zhang, Min Tan, and Junzhi Yu, *Fellow, IEEE*

***Abstract*—This article confronts the formation control problem for a multirobotic fish system with event-triggered communication mechanism. A 3-D distributed formation control framework is proposed to drive the robotic fish agents to an anticipated configuration aligning with a moving target. In particular, a consensus-based formation control law is intended to realize the two-stage formation control process. Taking the energy-constrained occasions into consideration, the communication structure and event-triggered protocols are initially tailored. Meanwhile, the Lyapunov function is employed and the globally asymptotic stability of the proposed method is fully demonstrated. Afterwards, making use of the local measurements of triggering times, the unscented Kalman filter is introduced and a novel model-based event-triggered mechanism is put forward to further mitigate otiose communication consumption. Finally, adequate simulations and experiments are carried out to verify the effectiveness and robustness of the proposed scheme. Thereby, the proposed formation control frame offers great potential for future practical marine operations of the underwater multiagent systems.**

***Index Terms*—Formation control, model-based event-triggered mechanism (ETM), robotic fish, underwater multiagent system.**

Manuscript received 29 September 2022; revised 23 November 2022; accepted 15 December 2022. Date of publication 4 January 2023; date of current version 8 May 2023. This work was supported in part by the National Natural Science Foundation of China under Grant 62033013, Grant 62022090, Grant 61973303, and Grant U1909206, and in part by Youth Innovation Promotion Association CAS under Grant 2019138. *(Corresponding author: Zhengxing Wu.)*

Shijie Dai and Pengfei Zhang are with the School of Artificial Intelligence, University of Chinese Academy of Sciences, Beijing 100049, China, and also with the State Key Laboratory of Management and Control for Complex Systems, Institute of Automation, Chinese Academy of Sciences, Beijing 100190, China (e-mail: daishijie2018@ia.ac.cn; zhangpengfei2017@ia.ac.cn).

Zhengxing Wu and Min Tan are with the State Key Laboratory of Management and Control for Complex Systems, Institute of Automation, Chinese Academy of Sciences, Beijing 100190, China (e-mail: zhengxing.wu@ia.ac.cn; min.tan@ia.ac.cn).

Junzhi Yu is with the State Key Laboratory of Management and Control for Complex Systems, Institute of Automation, Chinese Academy of Sciences, Beijing 100190, China, and also with the State Key Laboratory for Turbulence and Complex System, Department of Advanced Manufacturing and Robotics, BIC-ESAT, College of Engineering, Peking University, Beijing 100871, China (e-mail: junzhi.yu@ia.ac.cn).

Color versions of one or more figures in this article are available at https://doi.org/10.1109/TIE.2022.3232659.

Digital Object Identifier 10.1109/TIE.2022.3232659

I. Introduction

COMPARED with a single autonomous underwater vehicle (AUV), more underwater multiagent robotic systems come to the fore in recent years, which are endowed with the capability to make up defects in low sensor accuracy and limited operating abilities [1], [2]. Possessing better performance in complex marine occasions, these multiagent systems are widely used in mapping, geoscience, security, and biological discovery [3], [4]. Concerned as one of essential research fields for the multiagent system, formation control is entailed in several marine operations, such as exploring, patrolling, detecting, rescuing, and hunting [5], [6].

To impel the multiagent system to an anticipate configuration globally, plentiful researches have been made to construct several formation control laws, including leader–follower schemes, consensus-based methods, virtual structure strategies, and artificial potential field techniques [7], [8], [9], [10]. For instance, He et al. designed an adaptive formation controller based on the leader–follower schemes for unmanned surface vehicles, where collision between each vehicle and its leader was avoided [11]. Yan et al. proposed a formation generation algorithm combining a virtual structure and artificial potential field, which provided a sufficient accuracy for formation keeping and formation transformation [12]. Regarded as a spacial consensus problem, the formation control task was solved by Maghenem et al. for groups of nonholonomic mobile robots via a decentralized consensus-based formation controller, while the stability of the consensus set was strictly proved [13]. Wang et al. investigated the impact of nonidentical input delay during the formation process and a fixed-time consensus-based formation protocol was constructed [14].

Different from common formation control tasks, most AUVs confront energy-constrained occasions during marine assignments [15], [16]. In view of these cases, the event-triggered mechanism (ETM) decides interaction times among neighbors when only deemed necessary and proves advantageous to optimize the communication structure [17], [18], [19]. Cheng et al. considered the formation control problem for linear networked agents where an edge-based event-triggered protocol was constrained to reduce the bandwidth need of communication [20]. Meng et al. investigated the consensus problem for nonlinear second-order multiagent systems and an event-triggered

distributed control law was designed to achieve semiglobal robust leaderless consensus [21]. By virtue of state estimation schemes including a distributed Lyapunov-based model predictive controller and the extended state observer (ESO)-based auxiliary control law, Wei et al. improved the formation performance of the multi-AUV system with online optimization [22]. Yang et al. proposed a model-based edge-event-triggered containment control protocol to solve the energy conservation tradeoff between actuators and sensors [23].

It is pretty challenging to perform the deployment tasks for underwater multiagent systems. Jaffe et al. introduced a swarm of mini autonomous underwater explorers (M-AUEs), which owned their novel capability for measuring submesoscale dynamics [24]. Berlinger et al. [25] proposed a fish-inspired miniature underwater robot swarm and finished several 3-D collective behaviors through implicit communication. Focusing on the multirobotic fish system made up of several bionic robotic fish, the unique locomotion pattern and compact assembly space constraint the battery capacity of a single agent, which places imperious demands in communication energy conservation [26]. Hence, sustaining a tradeoff between the control performance and satisfactory resource consumption, formation control problem is more complicated for the multirobotic fish system. In previous work, the researches rarely focused on practical assignments for multirobotic fish systems. Besides, some existing consensus-based formation control researches were carried out with vital states of adjacent agents monitored continuously, which ran counter to the event-triggered conception and might not pertain for practical implementations. What is more, communication restriction and resource consumption should be taken into account for the formation control of a multirobot fish system.

Motivated by these observations, this article aims to realize the formation control task for a multirobotic fish system. The main contributions of this article are threefold.

1) A novel distributed formation control framework is established for the multirobotic fish system. Catering for the communication mode of the robotic fish, a node-based ETM protocol is adopted with the distributed consensus-based control protocol. Coping with more practical implementation occasions, a moving leader with aperiodically accessible states is considered and an error dynamic system is constructed for the formation task of the robotic fish with nonlinear dynamics.
2) A new consensus criterion is employed with the Lyapunov function and the event-triggered protocols are initially tailored to guarantee the convergence of the proposed method. Without continuous monitoring of adjacent states, the framework operates fully based on local measurements.
3) The unscented Kalman filter (UKF) is introduced to construct a novel distributed model-based ETM. Based on aperiodic measurements, the communication logical is further optimized and the triggering times are ulteriorly cut down.

Finally, various simulations and experiments on a real multirobotic fish system are carried out to show advantages of the proposed methods.

The rest of this article is organized as follows. Section II discusses the preliminaries and formulation of the formation control task. Section III presents the proposed event-triggered formation control frame. Simulation analysis and experimental verification are introduced in Section IV. Finally, Section V concludes this article.

II. Preliminaries and Problem Formulation

A. Algebraic Graph Theory

A multirobotic fish system with an N robotic fish is considered in this work. To describe the communication topology of the multirobotic fish system, an undirected digraph $\mathcal{G} = (\mathcal{V}, \mathcal{E})$ is utilized with a vertex set $\mathcal{V} = \{1, 2, \ldots, N\}$ and an edge set $\mathcal{E} \subseteq \mathcal{V} \times \mathcal{V}$. $\mathcal{A}$ is a weighted adjacency matrix where $\mathcal{A} = [a_{ij}]_{N\times N}$. $(i, j) \in \mathcal{E}$ means two agents i and j are associated with each other with $a_{ij} = 1$, and $a_{ij} = 0$ otherwise. Here, self-edge is not permitted, so $(i, i) \notin \mathcal{E}$ for any $i \in \mathcal{V}$. Meanwhile, the degree matrix is denoted as $\mathcal{D} = \text{diag}\{d_1, d_2, \ldots, d_N\}$, where $d_i = \sum_{j=1}^{N} a_{ij}$. The Laplacian matrix $\mathcal{L} = [l_{ij}]_{N\times N}$ is defined as $\mathcal{L} = \mathcal{D} - \mathcal{A}$. It is worth reminding that hereafter $\|\cdot\|$ represents the Euclidean norm of a vector or the spectral norm of a matrix. $\otimes$ stands for the Kronecker product. $I_n \in \mathbb{R}^{n\times n}$ and $O_n \in \mathbb{R}^{n\times n}$ denote identity matrix and null matrix, respectively, while two typical vectors are symbolized as $\mathbf{1}_N = [1, \ldots, 1]^T_{N\times 1}$ and $\mathbf{0}_N = [0, \ldots, 0]^T_{N\times 1}$.

Lemma 1: The Laplacian matrix $\mathcal{L}$ of $\mathcal{G}$ is symmetric and positive semidefinite. If $\mathcal{G}$ is connected, its eigenvalues are sorted in ascending order as $0 = \lambda_1(\mathcal{L}) \leq \lambda_2(\mathcal{L}) \leq \cdots \leq \lambda_N(\mathcal{L}) = \lambda_{\max}(\mathcal{L})$.

B. Problem Statement

With aforementioned communication topology, each robotic fish knows its own states and shares the states among neighbors if necessary. Furthermore, the formation control task can be depicted by a two-stage process as follows:

1) *Formation producing stage:* Each robotic fish in the multirobotic fish system makes quick convergence to set up a reliable communication topology, which constitutes a predefined shape globally.
2) *Formation keeping stage:* To guide the whole system to a preconcerted area, a moving target is introduced as a virtual leader. Centered on the moving target, agents in the system swim while keeping pace with it to present a dynamic formation configuration.

It is assumed that formation configuration is defined in a 2-D space, represented by $\Delta = [\delta_{ij}]$. Thus, a desired formation is delineated for the agent i with a virtual position $\delta_i \in \mathbb{R}^n$, where $\delta_{ij} = \delta_i - \delta_j$ and $n = 3$ is the dimension of the virtual position. A position vector $\eta_i = [x_i, y_i, \psi_i]^T$ and a speed vector $\upsilon_i = [\dot{x}_i, \dot{y}_i, \dot{\psi}_i]^T$ are introduced for the agent i with respect to (w.r.t.) the world coordinate frame $\{C_w\}$, where $p_i = [x_i, y_i]^T$

is a 2-D coordinate and ψ_i represents the yaw angle, respectively. Similarly, states of the moving target are expressed as $\eta_l = [x_l, y_l, \psi_l]^T$ and $\upsilon_l = [\dot{x}_l, \dot{y}_l, \dot{\psi}_l]^T$. The moving target is considered as the locomotion center of the multirobotic fish system, where δ_l is the origin of coordinates of Δ. Therefore, the formation control problem can be specified as follows.

Definition 1: Agents achieve the desired formation with an anticipated configuration if equations exit for the agent i that

$$\lim_{t\to\infty} \|\eta_i(t) - \eta_j(t) - \delta_{ij}\| = \mathbf{0}_n, (i,j) \in \mathcal{E} \tag{1}$$

$$\lim_{t\to\infty} \|\eta_i(t) - \eta_l(t) - \delta_{il}\| = \mathbf{0}_n \tag{2}$$

where $\delta_{il} = \delta_i - \delta_l$ is introduced to denote a desired relative position to the center.

The formation error ε_e is introduced to measure a deviation of the formation process, which is formalized as follows:

$$\varepsilon_e = \sum_{i\in\mathcal{V}} \Phi \|\eta_l(t) + \delta_{il} - \eta_i(t)\| \tag{3}$$

where $\Phi \in \mathbb{R}^{n\times n}$ is a diagonal normalized matrix.

Remark 1: At least one of the agents can detect the leader and broadcast its states through communication topology $\mathcal{G}$ on demand, in the meanwhile, a spanning tree is constructed from this agent as a root node. $\mathcal{W} = \text{diag}\{w_1, w_2, \ldots, w_N\}$ is introduced to describe connections between the leader and other agents. In other words, once the agent i can receive states of the leader, it is denoted that $w_i = 1$.

C. Dynamic Model

To facilitate description of the formation process, locomotion of the robotic fish in 2-D space is focused and corresponding dynamic model is presented w.r.t. the body-fixed moving coordinate frame $\{C_{bi}\}$ for every robotic fish with a homogeneous form as follows [27]:

$$M_i\dot{\nu}_i = -C_i(\nu_i)\nu_i - D_i(\nu_i)\nu_i + {}^b\tau_i \tag{4}$$

where the generalized force is expressed as ${}^b\tau_i = [\tau_{ui}, \tau_{vi}, \tau_{ri}]^T$, including surge force τ_{ui}, sway force τ_{vi}, and yaw moment τ_{ri}. The corresponding generalized speed is denoted by $\nu_i = [u_i, v_i, r_i]^T$. $M_i = \text{diag}\{m_{11}, m_{22}, m_{33}\}$ combines the inertia matrix and the added inertia matrix. $C_i(\nu_i)$ groups the Coriolis-centrifugal force generated by extra mass, while $D_i(\nu_i)$ is the hydrodynamic damping term.

By substituting $\upsilon_i(t)$ into (4), aforementioned dynamic model is represented w.r.t. $\{C_w\}$ as follows:

$$\begin{aligned} M_i\dot{\upsilon}_i &= M_i\Omega R_{bi}\nu_i - M_iR_{bi}M_i^{-1}C_i\nu_i \\ &\quad - M_iR_{bi}M_i^{-1}D_i\nu_i + M_iR_{bi}M_i^{-1}{}^b\tau_i \\ &= M_i\Omega R_{bi}\nu_i - R_{bi}C_i\nu_i - R_{bi}D_i\nu_i + R_{bi}{}^b\tau_i = f_i + \tau_i \end{aligned} \tag{5}$$

where $m_{11} = m_{22}$ is assumed to derive that $M_iR_{bi}M_i^{-1} = R_{bi}$ and $f_i = M_i\Omega R_{bi}\nu_i - R_{bi}C_i\nu_i - R_{bi}D_i\nu_i$. $\tau_i = R_{bi}{}^b\tau_i = [\tau_{xi}, \tau_{yi}, \tau_{ri}]^T$ is the generalized force w.r.t. $\{C_w\}$. Ω is a skew-symmetric matrix, and R_{bi} is the rotation matrix of $\{C_{bi}\}$ w.r.t. $\{C_w\}$, both of which are denoted by

$$\Omega = \begin{bmatrix} 0 & -\dot{\psi}_i & 0 \\ \dot{\psi}_i & 0 & 0 \\ 0 & 0 & 0 \end{bmatrix}, R_{bi} = \begin{bmatrix} \cos\psi_i & -\sin\psi_i & 0 \\ \sin\psi_i & \cos\psi_i & 0 \\ 0 & 0 & 1 \end{bmatrix}. \tag{6}$$

In a word, the nonlinear dynamic model of the agent i and the leader in the multirobotic fish system can be formalized by

$$\begin{cases} \dot{\eta}_i(t) = \upsilon_i(t) \\ M_i\dot{\upsilon}_i(t) = f_i(t) + \tau_i(t) \end{cases}, \begin{cases} \dot{\eta}_l(t) = \upsilon_l(t) \\ M_l\dot{\upsilon}_l(t) = f_l(t) \end{cases} \tag{7}$$

where the leader is expressed by an autonomous system, which is delineated by an implicit expression $f_l(t)$. Assuming that locomotion of the leader is also restricted as other followers, an upper limit is expressed as $\sup_{i\in\mathcal{V}}\{\|f_i(t) - f_l(t)\|\} = \Delta_f$.

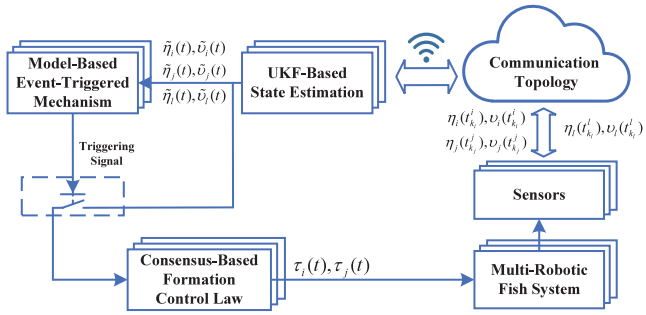

Fig. 1. Overview of the event-triggered formation control framework.

III. Event-Triggered-Based Formation Control

Fig. 1 depicts an overview of the proposed formation control framework. In particular, agents in the multirobotic fish system collect measurements in real time and broadcast pivotal states through the communication topology. Based on the intermittent interactions, the UKF is introduced to construct a novel distributed model-based ETM and decide when to broadcast current states. Furthermore, the consensus-based formation control law is established by local measurements, which drive the whole system to a predefined configuration. Therefore, the multirobotic fish system can keep an anticipated formation while mitigating unnecessary wastes of communication resources by this event-triggered formation control framework.

A. Event-Triggered Protocol and Formation Control Law

The formation control problem aims to produce a predefined configuration while making the whole system pursuit toward the moving target. However, in view of the practical application, the situation is pretty grim in the presence of hostile underwater environment. In other words, it is crucial for the multirobotic fish system to evaluate interaction messages and transfer information selectively. Meanwhile, the accuracy of the formation is not a primary objective for underwater exploration, which makes it possible to reduce energy consumption by sacrificing acceptable control precision. Therefore, taking aforementioned

questions into consideration, an ETM is proposed to deal with the formation control problem in this work.

According to different communication patterns, the ETM can be classified into node-based algorithm and edge-based algorithm. The edge-based method sets up a one-to-one interaction channel between two linked nodes, which is customized but computationally burdensome. Relatively, the node-based algorithm has a more concise form to establish a one-to-many correspondence, which is in accordance with the commonly used communication equipment of the robotic fish. Hence, a node-based ETM protocol is adopted. Once the event detector determines a triggering occasion, robotic fish, acted as node i, broadcasts its states $\eta_i(t^i_{k_i})$ and $\upsilon_i(t^i_{k_i})$ to all its neighbors in $\mathcal{E}$, where the sequence of triggering times is represented as $\{t^i_0, t^i_1, \ldots, t^i_{k_i}, \ldots\}$. $t^i_{k_i}$ is represented by

$$t^i_{k_i} = \inf\left\{t > t^i_{k_i-1} : \Gamma_i(t) \geq 0\right\} \tag{8}$$

where $\Gamma_i(t)$ is the event-triggered function. It means once $\Gamma_i(t) < 0$ is violated, the state information is published and triggering time $t^i_{k_i}$ is recorded. Trigger error vectors are defined as deviations of the states between the triggering time and current time, denoted as $e_{\eta i}(t) = \eta_i(t^i_{k_i}) - \eta_i(t)$ and $e_{\upsilon i}(t) = \upsilon_i(t^i_{k_i}) - \upsilon_i(t)$.

Note that in some existing literature, states of the neighbors are acquired from an extra communication link or an ask mechanism [28], [29], [30]. In addition, states of the leader are assumed available at any time in some related works [31], [32]. However, with regard to a distributed control system, these protocols aggravate the burden of network transmission and energy consumption, which run counter to the event-triggered method. In contrast, communication and states sharing among agents are only carried out at triggering times in this work, where the control laws and event-triggered functions are designed based on available local measurements. Moreover, states of the leader are also aperiodically accessible to meet the practical uses based on a standalone event-triggered function.

In line with the proposed event-triggered protocol, a consensus-based control law for the agent i is designed as

$$\begin{aligned}\tau_i(t) = &\sum_{j\in\mathcal{V}} a_{ij}\sigma\Phi\left[\eta_j(t^j_{k_j}) - \eta_i(t^i_{k_i}) - \delta_{ji} + \upsilon_j(t^j_{k_j}) - \upsilon_i(t^i_{k_i})\right] \\ &+ w_i\sigma_l\Phi\left[\eta_l(t^l_{k_l}) - \eta_i(t^i_{k_i}) - \delta_{li} + \upsilon_l(t^l_{k_l}) - \upsilon_i(t^i_{k_i})\right]\end{aligned} \tag{9}$$

where σ and σ_l are positive coefficients.

By introducing $\hat{\eta}_i(t) = \eta_i(t) - \eta_l(t) - \delta_{il}$ and $\hat{\upsilon}_i(t) = \upsilon_i(t) - \upsilon_l(t)$, the control law in (9) can be further deduced by

$$\begin{aligned}\tau_i(t) = &\sum_{j\in\mathcal{V}} a_{ij}\sigma\Phi[e_{\eta j}(t) + \hat{\eta}_j(t) + e_{\upsilon j}(t) + \hat{\upsilon}_j(t)] \\ &- \sum_{j\in\mathcal{V}} a_{ij}\sigma\Phi[e_{\eta i}(t) + \hat{\eta}_i(t) + e_{\upsilon i}(t) + \hat{\upsilon}_i(t)] \\ &- w_i\sigma_l\Phi[e_{\eta i}(t) + \hat{\eta}_i(t) + e_{\upsilon i}(t) + \hat{\upsilon}_i(t) - e_{\eta l}(t) - e_{\upsilon l}(t)] \\ = &-\sum_{j\in\mathcal{V}} l_{ij}\sigma\Phi[e_{\eta j}(t) + \hat{\eta}_j(t) + e_{\upsilon j}(t) + \hat{\upsilon}_j(t)] \\ &- w_i\sigma_l\Phi[e_{\eta i}(t) + \hat{\eta}_i(t) + e_{\upsilon i}(t) + \hat{\upsilon}_i(t) - e_{\eta l}(t) - e_{\upsilon l}(t)].\end{aligned} \tag{10}$$

An error dynamic system is constructed combining (7) and (10). Without loss of generality, it is assumed that $M_l = M_i$, and the final system is given by

$$\begin{cases}\dot{\hat{\eta}}_i(t) = \hat{\upsilon}_i(t) \\ M_i\dot{\hat{\upsilon}}_i(t) = -\sum_{j\in\mathcal{V}} l_{ij}\sigma\Phi[e_{\eta j}(t) + \hat{\eta}_j(t) + e_{\upsilon j}(t) + \hat{\upsilon}_j(t)] \\ -w_i\sigma_l\Phi[e_{\eta i}(t) + \hat{\eta}_i(t) + e_{\upsilon i}(t) + \hat{\upsilon}_i(t)] \\ +w_i\sigma_l\Phi[e_{\eta l}(t) + e_{\upsilon l}(t)] + f_i - f_l.\end{cases} \tag{11}$$

Considering all of agents in the multirobotic fish system and introducing $M = \text{diag}\{M_1, M_2, \ldots, M_N\}$, $\hat{\eta} = [\hat{\eta}_1^T(t), \hat{\eta}_2^T(t), \ldots, \hat{\eta}_N^T(t)]^T$, $\hat{\upsilon} = [\hat{\upsilon}_1^T(t), \hat{\upsilon}_2^T(t), \ldots, \hat{\upsilon}_N^T(t)]^T$, $F = [f_1^T, f_2^T, \ldots, f_N^T]^T$, $e_\eta = [e_{\eta 1}^T(t), e_{\eta 2}^T(t), \ldots, e_{\eta N}^T(t)]^T$, and $e_\upsilon = [e_{\upsilon 1}^T(t), e_{\upsilon 2}^T(t), \ldots, e_{\upsilon N}^T(t)]^T$, the error dynamic model can be reduced concisely by

$$\begin{bmatrix} I_{Nn} & O_{Nn} \\ O_{Nn} & M \end{bmatrix}\dot{\hat{\xi}} = K\hat{\xi} + Je + Ne_l + H \tag{12}$$

where $\hat{\xi} = [\hat{\eta}^T, \hat{\upsilon}^T]^T$, $e_l = [\mathbf{1}_N^T \otimes e_{\eta l}(t), \mathbf{1}_N^T \otimes e_{\upsilon l}(t)]^T$, and $e = [e_\eta^T(t), e_\upsilon^T(t)]^T$. K, J, N, and H are parameterized as

$$K = \begin{bmatrix} O_{Nn} & I_{Nn} \\ -(\sigma\mathcal{L} + \sigma_l\mathcal{W}) \otimes \Phi & -(\sigma\mathcal{L} + \sigma_l\mathcal{W}) \otimes \Phi \end{bmatrix} \tag{13}$$

$$J = \begin{bmatrix} O_{Nn} & O_{Nn} \\ -(\sigma\mathcal{L} + \sigma_l\mathcal{W}) \otimes \Phi & -(\sigma\mathcal{L} + \sigma_l\mathcal{W}) \otimes \Phi \end{bmatrix} \tag{14}$$

$$N = \begin{bmatrix} O_{Nn} & O_{Nn} \\ \sigma_l\mathcal{W} \otimes \Phi & \sigma_l\mathcal{W} \otimes \Phi \end{bmatrix}, H = \begin{bmatrix} \mathbf{0}_{Nn} \\ F - \mathbf{1}_N \otimes f_l \end{bmatrix}. \tag{15}$$

Therefore, as long as the stability of the error dynamic system in (12) is proved, the formation error in (3) is converged. In a word, the multirobotic fish system can keep an anticipated formation while pursuing toward the virtual leader.

B. Stability Analysis and Event-Triggered Function

In order to analyze the stability of the error dynamic system in (12), a Lyapunov function is established as follows:

$$V_{\hat{\xi}} = \frac{1}{2}\hat{\xi}^T P\hat{\xi} \tag{16}$$

where $P \in \mathbb{R}^{2Nn\times 2Nn}$ is a positive definite matrix, which is further represented as

$$P = \begin{bmatrix} (2\sigma\mathcal{L} + 2\sigma_l\mathcal{W}) \otimes \Phi & I_{Nn} \\ I_N \otimes \Phi & I_{Nn} \end{bmatrix}\begin{bmatrix} I_{Nn} & O_{Nn} \\ O_{Nn} & M \end{bmatrix}. \tag{17}$$

Derivative of the Lyapunov function is derived by

$$\begin{aligned}\dot{V}_{\hat{\xi}} = &\hat{\xi}^T\begin{bmatrix} (2\sigma\mathcal{L} + 2\sigma_l\mathcal{W}) \otimes \Phi & I_{Nn} \\ I_N \otimes \Phi & I_{Nn} \end{bmatrix}\begin{bmatrix} I_{Nn} & O_{Nn} \\ O_{Nn} & M \end{bmatrix}\dot{\hat{\xi}} \\ = &-\hat{\eta}^T(\sigma\mathcal{L} + \sigma_l\mathcal{W}) \otimes \Phi\hat{\eta} + \hat{\eta}^T Q + \hat{\upsilon}^T Q \\ &-\hat{\upsilon}^T(\sigma\mathcal{L} + \sigma_l\mathcal{W} - I_N) \otimes \Phi\hat{\upsilon}\end{aligned} \tag{18}$$

where Q is expressed as follows:

$$\begin{aligned} Q = & -(\sigma\mathcal{L}+\sigma_l\mathcal{W})\otimes\Phi(e_\eta+e_\upsilon) \\ & +\sigma_l\mathcal{W}\otimes\Phi(\mathbf{1}_N\otimes e_{\eta l}+\mathbf{1}_N\otimes e_{\upsilon l}) \\ & +F-\mathbf{1}_N\otimes f_l. \end{aligned} \tag{19}$$

Although $\hat{\eta}_i(t)$ and $\hat{\upsilon}_i(t)$ are propitious to measure deviations of the error dynamic system, both of them are unavailable in practice to agent i. Accordingly, some available measurements are introduced in this work as $\overline{\eta}_i(t)=\eta_i(t^i_{k_i})-\eta_l(t^l_{k_l})-\delta_{il}$ and $\overline{\upsilon}_i(t)=\upsilon_i(t^i_{k_i})-\upsilon_l(t^l_{k_l})$, where following relations are constructed as

$$\begin{aligned} \|\overline{\eta}+\overline{\upsilon}\| &= \|\hat{\eta}+\hat{\upsilon}+e_\eta+e_\upsilon-e_{\eta l}-e_{\upsilon l}\| \\ &\le \|\hat{\eta}+\hat{\upsilon}\|+\|e_\eta+e_\upsilon\|+\|e_{\eta l}+e_{\upsilon l}\|. \end{aligned} \tag{20}$$

On account of available local measurements, different forms of event-triggered functions are presented for leader agent and the others, which are established, respectively, as

$$\begin{aligned} \Gamma_l(t) = & (\|\sigma_l\mathcal{W}\|\|\Phi\|\|\mathbf{1}_N\|+\beta(\|\mathcal{D}\|+\|\mathcal{W}\|))\|e_{\eta l}(t)+e_{\upsilon l}(t)\| \\ & -\beta\lambda_l\sum_{j\in\mathcal{V}}w_j\|\overline{\eta}_j(t)+\overline{\upsilon}_j(t)\| \end{aligned} \tag{21}$$

$$\begin{aligned} \Gamma_i(t) = & (\|\sigma\mathcal{L}+\sigma_l\mathcal{W}\|\|\Phi\|+\beta(\|\mathcal{D}\|+\|\mathcal{W}\|))\|e_{\eta i}(t)+e_{\upsilon i}(t)\| \\ & +\Delta_f-\beta\lambda_i\sum_{j\in\mathcal{V}}a_{ij}\|\overline{\eta}_j(t)+\overline{\upsilon}_j(t)\| \end{aligned} \tag{22}$$

where β is a positive coefficient. $\lambda_i=\lambda_l\le 1$ are positive threshold parameters.

Since $\Gamma_i(t)<0$ is guaranteed, a further deduction of (22) is given that

$$\begin{aligned} & \sum_i(\|\sigma\mathcal{L}+\sigma_l\mathcal{W}\|\|\Phi\|+\beta(\|\mathcal{D}\|+\|\mathcal{W}\|))\|e_{\eta i}(t)+e_{\upsilon i}(t)\| \\ & <\sum_i\left[-\|f_i-f_l\|+\beta\lambda_i\sum_{j\in\mathcal{V}}a_{ij}\|\overline{\eta}_j(t)+\overline{\upsilon}_j(t)\|\right] \\ & \leqslant \sum_i\beta\lambda_i\sum_{j\in\mathcal{V}}a_{ij}\|\overline{\eta}_j(t)+\overline{\upsilon}_j(t)\|-\sum_i\|f_i-f_l\| \\ & =\sum_i\beta d_i\lambda_i\|\overline{\eta}_i(t)+\overline{\upsilon}_i(t)\|-\sum_i\|f_i-f_l\|. \end{aligned} \tag{23}$$

Similarly, it is derived from $\Gamma_l(t)<0$ that

$$\begin{aligned} & (\|\sigma_l\mathcal{W}\|\|\Phi\|\|\mathbf{1}_N\|+\beta(\|\mathcal{D}\|+\|\mathcal{W}\|))\|e_{\eta l}(t)+e_{\upsilon l}(t)\| \\ & <\beta\lambda_l\sum_{j\in\mathcal{V}}g_j\|\overline{\eta}_j(t)+\overline{\upsilon}_j(t)\|\leqslant\beta\|\mathcal{W}\|\|\overline{\eta}+\overline{\upsilon}\|. \end{aligned} \tag{24}$$

By incorporating (24) into (23), it is deduced as

$$\begin{aligned} & (\|\sigma\mathcal{L}+\sigma_l\mathcal{W}\|\|\Phi\|)\|e_\eta+e_\upsilon\|+\|\sigma_l\mathcal{W}\|\|\Phi\|\|\mathbf{1}_N\|\|e_{\eta l}+e_{\upsilon l}\| \\ & +\|F-\mathbf{1}_N\otimes f_l\| \\ & <\beta(\|\mathcal{D}\|+\|\mathcal{W}\|)(\|\overline{\eta}+\overline{\upsilon}\|-\|e_\eta+e_\upsilon\|-\|e_{\eta l}+e_{\upsilon l}\|) \\ & \le\beta(\|\mathcal{D}\|+\|\mathcal{W}\|)\|\hat{\eta}+\hat{\upsilon}\|\le\beta(\|\mathcal{D}\|+\|\mathcal{W}\|)(\|\hat{\eta}\|+\|\hat{\upsilon}\|). \end{aligned} \tag{25}$$

Hence, those results are derived as follows:

$$\begin{aligned} \hat{\eta}^TQ &\le \|\hat{\eta}\|\|Q\|<\beta(\|\mathcal{D}\|+\|\mathcal{W}\|)\|\hat{\eta}\|(\|\hat{\eta}\|+\|\hat{\upsilon}\|) \\ &\le \frac{\beta(\|\mathcal{D}\|+\|\mathcal{W}\|)}{2}\left(3\|\hat{\eta}\|^2+\|\hat{\upsilon}\|^2\right) \end{aligned} \tag{26}$$

$$\begin{aligned} \hat{\upsilon}^TQ &\le \|\hat{\upsilon}\|\|Q\|<\beta(\|\mathcal{D}\|+\|\mathcal{W}\|)\|\hat{\upsilon}\|(\|\hat{\eta}\|+\|\hat{\upsilon}\|) \\ &\le \frac{\beta(\|\mathcal{D}\|+\|\mathcal{W}\|)}{2}\left(\|\hat{\eta}\|^2+3\|\hat{\upsilon}\|^2\right). \end{aligned} \tag{27}$$

As a consequence, further derivation of (18) is deduced finally as

$$\begin{aligned} \dot{V}_{\hat{\xi}} < & -[\lambda_{\min}(\sigma\mathcal{L}+\sigma_l\mathcal{W})\|\Phi\|-2\beta(\|\mathcal{D}\|+\|\mathcal{W}\|)]\|\hat{\eta}\|^2 \\ & -[\lambda_{\min}(\sigma\mathcal{L}+\sigma_l\mathcal{W}-I_N)\|\Phi\|-2\beta(\|\mathcal{D}\|+\|\mathcal{W}\|)]\|\hat{\upsilon}\|^2 \end{aligned} \tag{28}$$

where $\dot{V}_{\hat{\xi}}<0$ is proved and the error dynamic model is rendered globally asymptotic stable if β follows that

$$\beta\le\frac{\lambda_{\min}(\sigma\mathcal{L}+\sigma_l\mathcal{W}-I_N)\|\Phi\|}{2\|\mathcal{D}\|+2\|\mathcal{W}\|}. \tag{29}$$

Remark 2: For a neat and convenient implementation of the proposed event-based controllers, the event-triggered transmission method is utilized to realize a Zeno-freeness control [33]. In particular, the continuous-time system states are first sampled at discretized and equidistant instants of time $\{kh:k\in\mathbb{N}\}$ with a constant sampling period $h>0$. Therefore, it is clear that the event detectors only work at sampled time and the minimal interevent time $T_{\min}$ satisfies that $T_{\min}\ge h>0$, which eliminates the Zeno behavior.

C. Model-Based Event-Triggered Scheme

The event-triggered method compares current states and the last triggered states to determine the necessity of the next trigger, where the perception of adjacent states keeps still by the zero-order hold during the triggering interval. However, it is revealed that states of the robots change regularly in most cases, which means the traditional schemes overlook these prior knowledge. Accordingly, model-based event-triggered predictive control is constructed. Estimators of the system states on updated intervals are modeled instead of the zero-order hold. As a consequence, once estimated states converge to the real states, the triggering times are further reduced.

In this fashion, the agent i outfits d_i+1 state estimators for d_i neighbors and its own. It is worth reminding that for the same agent i, state estimators of different agents are preconfigured with consistent parameters. Meanwhile, the observations are totally obtained based on the updated time, which are synchronous for the linked agents. Hence, the estimation results keep pace

with each robot and the model-based event-triggered scheme is completely decentralized with local measurements.

Taking the spacial underwater application scenarios into consideration, it is pivotal to make a reliable estimation with limited and intermittent measurements. The Kalman filter shows its merits for data fusion between the estimations and the multisensor measurements to get the optimal state estimation. In light of this, an UKF is introduced to estimate the locomotion trends during the triggering interval [34]. Corresponding to last updated states $\eta_i(t^i_{k_i})$ and $\upsilon_i(t^i_{k_i})$ for the agent i, the estimated states are denoted by $\tilde{\eta}_i(t)$ and $\tilde{\upsilon}_i(t)$, respectively. The triggering error for the ETM gives way to the estimation error, represented by $e_{\eta i}(t) = \tilde{\eta}_i(t) - \eta_i(t)$ and $e_{\upsilon i}(t) = \tilde{\upsilon}_i(t) - \upsilon_i(t)$. Therefore, a valid UKF estimation cuts down communication demands by reducing the error function consisting of triggering errors, where the control law in (9) is updated as

$$\tau_i(t) = \sum_{j\in\mathcal{V}} a_{ij}\sigma\Phi\left[\tilde{\eta}_j(t) - \tilde{\eta}_i(t) - \delta_{ji} + \tilde{\upsilon}_j(t) - \tilde{\upsilon}_i(t)\right] + w_i\sigma_l\Phi\left[\tilde{\eta}_l(t) - \tilde{\eta}_i(t) - \delta_{li} + \tilde{\upsilon}_l(t) - \tilde{\upsilon}_i(t)\right]. \quad (30)$$

Meanwhile, the event-triggered functions in (21) and (22) are modified. Apart from $e_{\eta i}(t)$ and $e_{\upsilon i}(t)$, $\overline{\eta}_i(t)$ and $\overline{\upsilon}_i(t)$ are rewritten as $\overline{\eta}_i(t) = \tilde{\eta}_i(t) - \tilde{\eta}_l(t) - \delta_{il}$ and $\overline{\upsilon}_i(t) = \tilde{\upsilon}_i(t) - \tilde{\upsilon}_l(t)$, respectively. Note that once convergence of UKF is guaranteed, the model-based scheme does not affect the proven asymptotic stability of the event-triggered-based formation control law.

The main estimated state vector of the cycle k is denoted as $X_k = [\tilde{x}_i, \tilde{y}_i, \tilde{u}_i, \tilde{\psi}_i, \dot{\tilde{\psi}}_i]^T$ for the agent i, including 2-D positions $\tilde{x}_i$ and $\tilde{y}_i$, surge speed $\tilde{u}_i$, yaw angle $\tilde{\psi}_i$, and yaw angular speed $\dot{\tilde{\psi}}_i$. Composed of prediction and update, the whole iterative process of the UKF is formalized as follows.

By virtue of the unscented transformation, sigma points $\mathcal{X}_{k,m}$ are generated, where $m \in \{0, \ldots, n_\sigma\}$. $n_\sigma = 2n_a + 1$ and $n_a = 5$ is the dimension of X_k. Considering the constant turn rate and velocity (CTRV) model $f_p(\cdot)$, the estimated sigma point is denoted by

$$\mathcal{X}_{k+1|k,m} = f_p\left(\mathcal{X}_{k,i}, \nu_{k,i}\right) \quad (31)$$

where $\nu_{k,i}$ is the process noise.

Sigma points of cycle $k+1$ are estimated with the predicted state mean and covariance updated as

$$\mu_{k+1|k} = \sum_{m=1}^{n_\sigma} w_{\sigma,m}\mathcal{X}_{k+1|k,m}$$
$$P_{k+1|k} = \sum_{m=1}^{n_\sigma} w_{\sigma,m}\left(\mathcal{X}_{k+1|k,m} - \mu_{k+1|k}\right)\left(\mathcal{X}_{k+1|k,m} - \mu_{k+1|k}\right)^T \quad (32)$$

where $w_{\sigma,m}$ is the weight coefficient.

Combining the outputs from several sensors, measurements z_{k+1} are analyzed with predicted measurement mean $z_{k+1|k}$ and covariance $S_{k+1|k}$ as follows:

$$z_{k+1|k} = \sum_{m=1}^{n_\sigma} w_{\sigma,m}\mathcal{Z}_{k+1|k,m}$$
$$S_{k+1|k} = \sum_{m=1}^{n_\sigma} w_{\sigma,m}\left(\mathcal{Z}_{k+1|k,m} - z_{k+1|k}\right)\left(\mathcal{Z}_{k+1|k,m} - z_{k+1|k}\right)^T + R_{k+1} \quad (33)$$

where $\mathcal{Z}_{k+1|k,m}$ is the measurement sigma points vector and R_{k+1} is the measurement noise covariance. Furthermore, the cross-correlation $T_{k+1|k}$ and Kalman gain $K_{k+1|k}$ are deduced as

$$T_{k+1|k} = \sum_{m=1}^{n_\sigma} w_{\sigma,m}\left(\mathcal{X}_{k+1|k,m} - \mu_{k+1|k}\right)\left(\mathcal{Z}_{k+1|k,m} - z_{k+1|k}\right)^T$$
$$K_{k+1|k} = T_{k+1|k}S^{-1}_{k+1|k}. \quad (34)$$

Eventually, the estimated main state vector X_{k+1} and corresponding covariance P_{k+1} are updated as

$$X_{k+1} = \mu_{k+1|k} + K_{k+1|k}\left(z_{k+1} - z_{k+1|k}\right)$$
$$P_{k+1} = P_{k+1|k} - K_{k+1|k}S_{k+1|k}K^T_{k+1|k}. \quad (35)$$

Therefore, $\tilde{\eta}_i(t)$ and $\tilde{\upsilon}_i(t)$ are finally extracted from the UKF during the formation control task.

IV. Simulation Analysis and Experimental Results

A. Simulation Results of 3-D Formation Control Task

To illustrate the proposed formation control framework effectively, simulation environment is established in the robot operating system (ROS) and extensive simulations are carried out. The multirobotic fish system consists of three agents with a virtual leader. Agents scatter at different locations, whose initial positions are set as $\eta_l = [1.0, 1.0, 0]^T$, $\eta_1 = [1.5, 0.2, -0.5]^T$, $\eta_2 = [2.5, 0.2, 0.5]^T$, and $\eta_3 = [0.3, 1.8, 0]^T$. The anticipated configuration is set as $\delta_l = [0, 0, 0]^T$, $\delta_1 = [-0.46, -0.8, 0]^T$, $\delta_2 = [0.92, 0, 0]^T$, and $\delta_3 = [-0.46, 0.8, 0]^T$. Note that in the subsequent simulations, the communication topology $\mathcal{G}$ and $\mathcal{W}$ are strong connected, which means each robotic fish can interact with all the other agents and receive information about the virtual leader at triggering times. In the meanwhile, the leader can get states of others. The scheduled trajectory of the moving target is set as a 3-D helical path, which is parameterized by $x(\varpi) = 2.3 + 0.7\cos(\varpi)$, $y(\varpi) = 2 + 0.7\sin(\varpi)$, and $z(\varpi) = -\sin(\varpi/8 + \pi/16)$ with $\varpi \in [-0.5\pi, 4\pi]$. The control period and constant sampling time are set to $h = 0.08$ s. Afterwards, positive coefficients in the proposed control law are set as $\sigma = 5$ and $\sigma_l = 12$. The normalized matrix is chosen as $\Phi = \text{diag}\{1, 1, 0.2\}$. The locomotion restriction is set as $\Delta_f = 0.5$. Threshold parameters of the event-triggered functions are set as $\lambda_i = \lambda_l = 1$. To guarantee the stability of the proposed method, the coefficient is chosen as $\beta = 2$.

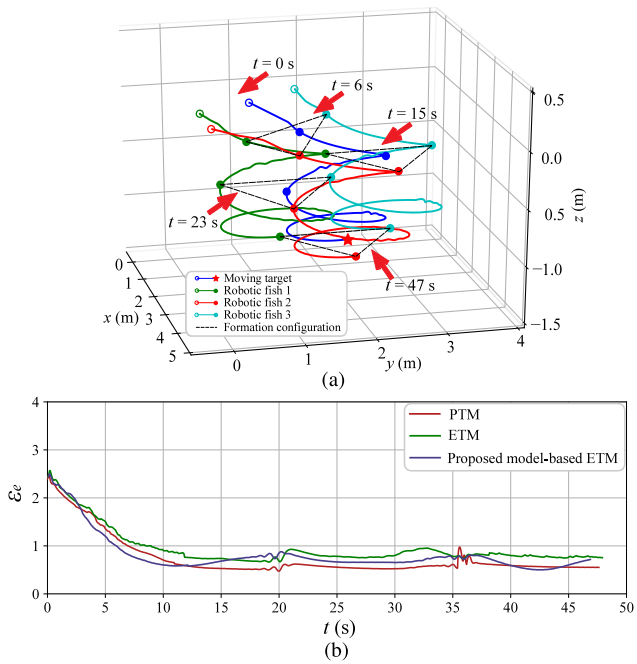

Fig. 2. Simulation results. (a) Formation control results with the proposed model-based ETM. (b) Comparisons of the formation errors with different triggering mechanisms.

TABLE I
TRIGGERING NUMBERS AND QUANTITATIVE ANALYSIS FOR SIMULATIONS

Items	Total triggering numbers				RMSE
	Leader	1	2	3	
PTM	931	931	931	931	0.667
ETM	157	602	580	590	0.791
Model-based ETM	193	345	409	301	0.682

Fig. 2(a) shows the simulation results with the consensus-based control law and proposed model-based ETM. In comparison, the periodic-triggered mechanism (PTM) is introduced to show the superiority of the event-triggered scheme, while the event-triggered formation control frame without state estimation is also employed. Fig. 2(b) depicts the formation control performance of different mechanisms. Furthermore, Table I records the total triggering numbers and exhibits the quantitative analysis, where root mean square error (RMSE) is utilized.

It reveals intuitively from the simulation results that the proposed consensus-based formation control law copes well with the 3-D formation control task. Albeit a complex helical trajectory of the moving target, the multirobotic fish system converges to a predefined shape at $t = 18$ s and keeps pace with an acceptable formation error gradually. Based on the same consensus-based mechanism, the other two with different triggering schemes also get ideal control performance.

Benefiting by frequent communication, PTM-based method owns the best performance with the lowest RMSE at 0.633. Nevertheless, with a negligible loss of formation performance less than 14%, two ETM-based methods, by contrast, dramatically reduce the triggering numbers, where over 32% communication consumption is saved. Specifically, according to the predictions by the UKF during two triggering intervals, the local knowledge to the neighbors stays closer to the truth. Hence, the triggering errors in the ETM further decline and more communication resources are economized during the aperiodic interactions. Therefore, the proposed consensus-based formation control method is validated to preserve a reliable formation control performance pursuing the moving target steadily. Moreover, the proposed model-based triggering mechanism can further regulate the communication intervals subtly with accessible local information, optimizing the communication logic while mitigating the unnecessary waste of communication resources. The stability and reliability are both demonstrated by adequate simulations.

TABLE II
TRIGGERING NUMBERS AND QUANTITATIVE ANALYSIS FOR EXPERIMENTS

Items	Total triggering numbers				RMSE
	Leader	1	2	3	
PTM	2100	2100	2100	2100	1.546
ETM	377	462	515	437	1.711
Model-based ETM	231	314	359	341	1.675

B. Experiments for Practical Implementations

To verify the stable performance of the proposed scheme, several practical experiments were carried out with a group of robotic remora developed in our group [35]. To constitute a multirobotic fish system, each agent owns a flexible 3-D locomotion ability, where the prototype of the robot and the real multirobotic fish system are shown in Fig. 3(a) and (b). Following experiments were conducted in the horizontal plane of a pool with 5-m long and 4-m wide. In the meanwhile, the parameters and procedures in the experimental scene settings kept the same with the simulations. The scheduled trajectory of the moving target is parameterized by $x(\varpi) = 2.3 + 0.7\cos(\varpi)$, $y(\varpi) = 2 + 0.7\sin(\varpi)$, and $z(\varpi) = 0$ with $\varpi \in [-0.5\pi, 4\pi]$. Keeping pace with the moving target, which is marked with a red star, the snapshot sequence of the formation control process is shown in Fig. 3(c).

Fig. 3(d) shows the experiment results with the proposed consensus-based control law and the model-based ETM. Similarly, the other two triggering mechanisms were carried out, where tracking errors with different triggering mechanisms are depicted in Fig. 3(e). Meanwhile, the triggering times fragment of the moving target and other agents with the proposed model-based ETM are intercepted in the first 16 s and depicted in Fig. 3(f). To further show the advantage of the proposed methods, the communication cases and formation control performance are analyzed in Table II. It is observed that the consensus-based method copes well with the dynamic formation control task. By setting up a connected communication topology, a robotic fish makes quick convergence to constitute the triangular configuration and the multirobotic fish system finishes the formation producing stage. Despite the target moving continuously with an unknown locomotion to each robotic fish, the multirobotic fish

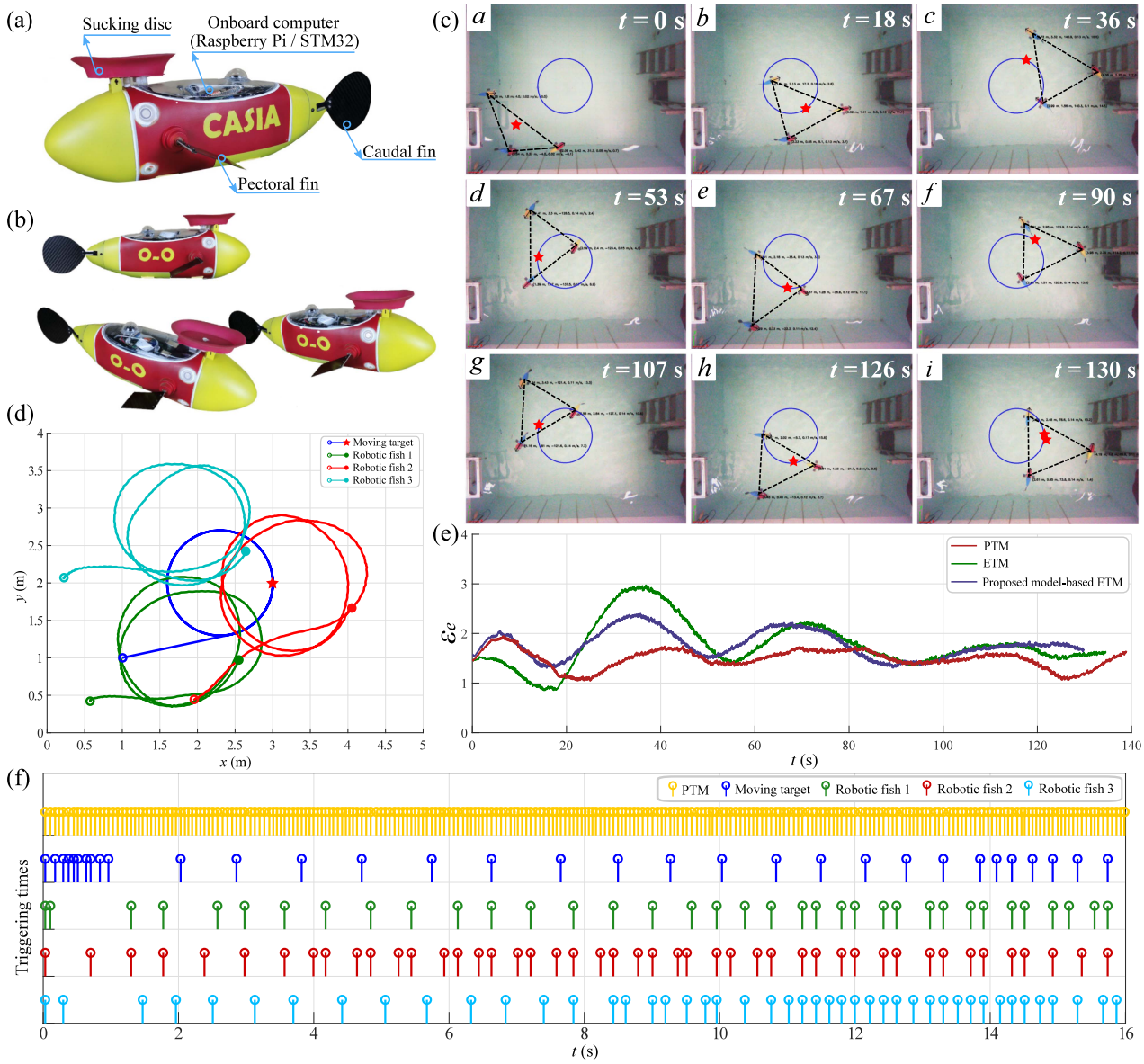

Fig. 3. Practical experiment results. (a) Prototype of the developed robotic remora. (b) Real multirobotic fish system with three agents. (c) Snapshot sequence for the formation control task. (d) Formation control results with the proposed model-based ETM. (e) Comparisons of the formation errors with different triggering mechanisms. (f) Triggering times fragment of the moving target and other agents with proposed model-based ETM.

system can keep pace with each other and gradually move toward the target based on aperiodic communication. Specifically, the proposed ETM shows its merits to reduce the triggering numbers. Contrasting with the basic interaction period at 0.08 s, the average communication periods of the multirobotic fish system are extended to 0.38 and 0.54 s for ETM and model-based ETM, respectively. It is worth noting that there is little difference between the RMSE of several triggering schemes, which means extensive resources are saved with inessential loss of control performance. Simultaneously, estimating by the UKF schemes, local measurements in the triggering times are fully utilized to get a probable tendency of the multirobotic fish system. Hence, more superfluous triggering times are cut down. Therefore, the proposed consensus-based method with the model-based ETM is validated to preserve a reliable formation control performance while mitigating the unnecessary waste of communication resources to a great extent.

C. Discussion

Based on the proposed consensus-based formation control law with model-based ETM, the multirobotic fish system keeps pace to construct an anticipate configuration and pursues the moving target with lower interaction consumption. In some existing literature [28], [29], [30], [31], [32], some defective assumptions were made during the simulation verification while the practical experiments were usually scarce. It is demonstrated clearly in aforementioned simulations and experiments that the proposed

formation control frame are distributed fully based on local measurements. Besides, the formation control setup is more general, where the leader has independent triggering mechanism and makes interactions with other agents in the meanwhile. Hence, the proposed framework can be implemented in more standard situations for practical application loaded on embedded software architectures. Moreover, on the basis of ETM, the proposed model-based ETM performs better to mitigate unnecessary waste of communication resources, further extending the average communication periods from 0.38 to 0.54 s. Taking the periodic intervals at 0.08 s, the communication channel capacity is largely released. It is reflected from the formation control performance that high-frequency communication is not necessarily favorable, especially near the equilibrium state. That is the reason why the proposed model-based ETM can avoid some superfluous control commands to get an ideal tradeoff between control performance and communication consumption, which is essential to underwater operations. To sum up, the feasibility and effectiveness of the proposed system are finally substantiated.

However, due to the intermittent acquisition about the local measurements, the UKF-based prediction is unable to make an acceptable estimation suffering from overstretched triggering intervals. The model-based ETM will reversely generate more triggering times at that moments. Several constraints may be considered to optimize the model-based mechanism. In addition, the expansibility hamper its implementation of the model-based ETM in practice. Once agents in the multirobot system have a sharp increase and the calculation is no longer superfluous, the distributed estimations are computationally burdensome. Some lightweight mechanisms may be utilized as substitutes.

V. Conclusion

In this article, we proposed a 3-D distributed formation control framework for a multirobotic fish system to constitute an anticipated configuration guided by a moving target. In order to formulate the control objectives, the formation control process was analyzed first. Thereafter, a novel formation control frame with the model-based ETM was proposed. In particular, the dynamic models of the leader and other agents were formalized, respectively. Sustaining a tradeoff between the control performance and communication consumption, independent event-triggered functions were presented for the leader and the others. According to the proposed consensus-based formation control protocol with the ETM, the Lyapunov function was established and the globally asymptotic stability was demonstrated in detail. Moreover, the UKF mechanism was introduced, and a novel model-based ETM was proposed to further reduce the triggering times. Finally, adequate simulations and experiments were carried out to validate the effectiveness of the proposed distributed formation control frame. In summary, the proposed formation control method was effective and executable in a formation control task for the multirobotic fish system, and also mitigated unnecessary communication wastes during the control process.

Future work will concentrate on unstructured environment with obstacles while exploring the formation transformation strategies with ETM.

References

[1] T. Schmickl et al., "CoCoRo-The self-aware underwater swarm," in *Proc. IEEE Conf. Self-Adapt. Self-Organ. Syst. Workshops*, Ann Arbor, MI, USA, Oct. 2011, pp. 120–126.

[2] T. Zhang, Y. Gou, J. Liu, T. Yang, and J. H. Cui, "UDARMF: An underwater distributed and adaptive resource management framework," *IEEE Internet Things J.*, vol. 9, no. 10, pp. 7196–7210, May 2022.

[3] Z. Peng, J. Wang, and D. Wang, "Distributed containment maneuvering of multiple marine vessels via neurodynamics-based output feedback," *IEEE Trans. Ind. Electron.*, vol. 64, no. 5, pp. 3831–3839, May 2017.

[4] G. Wang, C. Wang, Z. Ding, and Y. Ji, "Distributed consensus of nonlinear multi-agent systems with mismatched uncertainties and unknown high-frequency gains," *IEEE Trans. Circuits Syst. II, Exp. Briefs*, vol. 68, no. 3, pp. 938–942, Mar. 2021.

[5] L. Bayındır, "A review of swarm robotics tasks," *Neurocomputing*, vol. 172, pp. 292–321, Jan. 2016.

[6] J. Lin, Z. Miao, H. Zhong, W. Peng, Y. Wang, and R. Fierro, "Adaptive image-based leader-follower formation control of mobile robots with visibility constraints," *IEEE Trans. Ind. Electron.*, vol. 68, no. 7, pp. 6010–6019, Jul. 2021.

[7] Y. Cao, W. Yu, W. Ren, and G. Chen, "An overview of recent progress in the study of distributed multi-agent coordination," *IEEE Trans. Ind. Inform.*, vol. 9, no. 1, pp. 427–438, Feb. 2013.

[8] B. Das, B. Subudhi, and B. B. Pati, "Cooperative formation control of autonomous underwater vehicles: An overview," *Int. J. Autom. Comput.*, vol. 13, no. 3, pp. 199–225, 2016.

[9] J. Hu, H. Zhang, L. Liu, X. Zhu, C. Zhao, and Q. Pan, "Convergent multiagent formation control with collision avoidance," *IEEE Trans. Robot.*, vol. 36, no. 6, pp. 1805–1818, Dec. 2020.

[10] S. L. Dai, S. He, X. Chen, and X. Jin, "Adaptive leader-follower formation control of nonholonomic mobile robots with prescribed transient and steady-state performance," *IEEE Trans. Ind. Inform.*, vol. 16, no. 6, pp. 3662–3671, Jun. 2020.

[11] S. He, M. Wang, S. L. Dai, and F. Luo, "Leader-follower formation control of USVs with prescribed performance and collision avoidance," *IEEE Trans. Ind. Inform.*, vol. 15, no. 1, pp. 572–581, Jan. 2019.

[12] X. Yan, D. Jiang, R. Miao, and Y. Li, "Formation control and obstacle avoidance algorithm of a multi-USV system based on virtual structure and artificial potential field," *J. Mar. Sci. Eng.*, vol. 9, no. 2, pp. 1–17, Feb. 2021.

[13] M. Maghenem, A. Loría, E. Nuno, and E. Panteley, "Consensus-based formation control of networked nonholonomic vehicles with delayed communications," *IEEE Trans. Autom. Control*, vol. 66, no. 5, pp. 2242–2249, May 2021.

[14] C. Wang, H. Tnunay, Z. Zuo, B. Lennox, and Z. Ding, "Fixed-time formation control of multirobot systems: Design and experiments," *IEEE Trans. Ind. Electron.*, vol. 66, no. 8, pp. 6292–6301, Aug. 2019.

[15] Y. Yang, Y. Xiao, and T. Li, "A survey of autonomous underwater vehicle formation: Performance, formation control, and communication capability," *IEEE Commun. Surv. Tuts.*, vol. 23, no. 2, pp. 815–841, Apr.–Jun. 2021.

[16] Z. Yan, C. Zhang, W. Tian, and M. Zhang, "Formation trajectory tracking control of discrete-time multi-AUV in a weak communication environment," *Ocean Eng.*, vol. 245, 2022, Art. no. 110495.

[17] X. Ge, Q. L. Han, X. M. Zhang, and D. Ding, "Dynamic event-triggered control and estimation: A survey," *Int. J. Autom. Comput.*, vol. 18, no. 6, pp. 857–886, 2021.

[18] C. Peng and F. Li, "A survey on recent advances in event-triggered communication and control," *Inf. Sci.*, vol. 457, pp. 113–125, 2018.

[19] R. Wang et al., "Energy-management strategy of battery energy storage systems in DC microgrids: A distributed dynamic event-triggered H_∞ consensus control," *IEEE Trans. Syst., Man, Cybern., Syst.*, vol. 52, no. 9, pp. 5692–5701, Sep. 2022, doi: 10.1109/TSMC.2021.3129184.

[20] B. Cheng, Z. Wu, and Z. Li, "Distributed edge-based event-triggered formation control," *IEEE Trans. Cybern.*, vol. 51, no. 3, pp. 1241–1252, Mar. 2021.

[21] H. Meng, H. T. Zhang, Z. Wang, and G. Chen, "Event-triggered control for semiglobal robust consensus of a class of nonlinear uncertain multiagent systems," *IEEE Trans. Autom. Control*, vol. 65, no. 4, pp. 1683–1690, Apr. 2020.

[22] H. Wei, C. Shen, and Y. Shi, "Distributed Lyapunov-based model predictive formation tracking control for autonomous underwater vehicles subject to disturbances," *IEEE Trans. Syst., Man, Cybern., Syst.*, vol. 51, no. 8, pp. 5198–5208, Aug. 2021.
[23] J. Yang, F. Xiao, and J. Ma, "Model-based edge-event-triggered containment control under directed topologies," *IEEE Trans. Cybern.*, vol. 49, no. 7, pp. 2556–2567, Jul. 2019.
[24] J. S. Jaffe et al., "A swarm of autonomous miniature underwater robot drifters for exploring submesoscale ocean dynamics," *Nat. Commun.*, vol. 8, no. 1, pp. 1–8, 2017.
[25] F. Berlinger, M. Gauci, and R. Nagpal, "Implicit coordination for 3D underwater collective behaviors in a fish-inspired robot swarm," *Sci. Robot.*, vol. 6, no. 50, 2021, Art. no. eabd 8668.
[26] Z. Wu, J. Yu, Z. Su, M. Tan, and Z. Li, "Towards an Esox lucius inspired multimodal robotic fish," *Sci. China Inf. Sci.*, vol. 58, no. 5, pp. 1–13, 2015.
[27] S. Dai, Z. Wu, J. Wang, M. Tan, and J. Yu, "Barrier-based adaptive line-of-sight 3-D path-following system for a multi-joint robotic fish with sideslip compensation," *IEEE Trans. Cybern.*, to be published, doi: 10.1109/TCYB.2022.3155761.
[28] W. Zhu, Z. P. Jiang, and G. Feng, "Event-based consensus of multi-agent systems with general linear models," *Automatica*, vol. 50, no. 2, pp. 552–558, 2014.
[29] H. Li, X. Liao, T. Huang, and W. Zhu, "Event-triggering sampling based leader-following consensus in second-order multi-agent systems," *IEEE Trans. Autom. Control*, vol. 60, no. 7, pp. 1998–2003, Jul. 2015.
[30] N. Huang, Z. Duan, G. Wen, and Y. Zhao, "Event-triggered consensus tracking of multi-agent systems with Lur'e nonlinear dynamics," *Int. J. Control*, vol. 89, no. 5, pp. 1025–1037, 2016.
[31] W. Xu, D. W. Ho, L. Li, and J. Cao, "Event-triggered schemes on leader-following consensus of general linear multiagent systems under different topologies," *IEEE Trans. Cybern.*, vol. 47, no. 1, pp. 212–223, Jan. 2017.
[32] M. Zhao, C. Peng, W. He, and Y. Song, "Event-triggered communication for leader-following consensus of second-order multiagent systems," *IEEE Trans. Cybern.*, vol. 48, no. 6, pp. 1888–1897, Jun. 2018.
[33] C. Nowzari, E. Garcia, and J. Cortés, "Event-triggered communication and control of networked systems for multi-agent consensus," *Automatica*, vol. 105, pp. 1–27, 2019.
[34] S. Y. Chen, "Kalman filter for robot vision: A survey," *IEEE Trans. Ind. Electron.*, vol. 59, no. 11, pp. 4409–4420, Nov. 2012.
[35] P. Zhang, Z. Wu, Y. Meng, H. Dong, M. Tan, and J. Yu, "Development and control of a bioinspired robotic remora for hitchhiking," *IEEE/ASME Trans. Mechatronics*, vol. 27, no. 5, pp. 2852–2862, Oct. 2022.

Shijie Dai received the B.E. degree in automation from Harbin Engineering University, Harbin, China, in 2018. He is currently working toward the Ph.D. degree in control theory and control engineering with the Institute of Automation, Chinese Academy of Sciences, Beijing, China.

His current research interests include bioinspired underwater robots and intelligent control systems.

Zhengxing Wu (Senior Member, IEEE) received the B.E. degree in logistics engineering from the School of Control Science and Engineering, Shandong University, Jinan, China, in 2008, and the Ph.D. degree in control theory and control engineering from the Institute of Automation, Chinese Academy of Sciences (IACAS), Beijing, China, in 2015.

He is currently a Professor with the State Key Laboratory of Management and Control for Complex Systems, IACAS. His research interests include bioinspired robots and intelligent control systems.

Pengfei Zhang received the B.E. degree in detection, guidance, and control techniques from the School of Aeronautics and Astronautics, Central South University, Changsha, China, in 2017, and the Ph.D. degree in control theory and control engineering from the Institute of Automation, Chinese Academy of Sciences (IACAS), Beijing, China, in 2022.

His research interests include the intelligent control and environmental perception of bioinspired robotic fish.

Min Tan received the B.Sc. degree in control science and engineering from Tsinghua University, Beijing, China, in 1986, and the Ph.D. degree in control science and engineering from the Institute of Automation, Chinese Academy of Sciences (IACAS), Beijing, China, in 1990.

He is currently a Professor with the State Key Laboratory of Management and Control for Complex Systems, IACAS. He has authored and co-authored more than 200 papers in journals, books, and conference proceedings. His research interests include robotics and intelligent control systems.

Junzhi Yu (Fellow, IEEE) received the B.E. degree in safety engineering and the M.E. degree in precision instruments and mechanology from the North University of China, Taiyuan, China, in 1998 and 2001, respectively, and the Ph.D. degree in control theory and control engineering from the Institute of Automation, Chinese Academy of Sciences, Beijing, China, in 2003.

From 2004 to 2006, he was a Postdoctoral Research Fellow with the Center for Systems and Control, Peking University. He was an Associate Professor with the Institute of Automation, Chinese Academy of Sciences, in 2006, where he was a Full Professor in 2012. In 2018, he joined the College of Engineering, Peking University, as a Tenured Full Professor. His current research interests include intelligent robots, motion control, and intelligent mechatronic systems.